Correlated Multi-Symbol Modulation for Optical Fiber Transmissions

Yi Cai[1]*, Zhongxing Tian[1], Hansheng Xu[1], Huan Huang[1], Ji Huang[1], Xiaobin Dong[2], Bin Xia[2], Lin Sun[1], Xiaoling Wang[1], Gordon Ning Liu[1], and Gangxiang Shen[1]

[1] *School of Electronic and Information Engineering, Soochow University, Suzhou 215006, Jiangsu, China*

[2] *Fisilink Microelectronics Technology Co., Ltd, Wuhan 430000, Hubei, China*

**Corresponding author:* yicai@suda.edu.cn

***Abstract*—We review the progress of correlated multi-symbol modulation scheme for coherent optical fiber transmissions, which treats inter-symbol-interference as symbol correlation to achieve high spectral efficiency. We discuss key digital signal processing algorithms for implementing the scheme.**

Keywords*—*coherent optical communication, high spectral efficiency transmission, correlated modulation, maximum likelihood sequence detection

I. Introduction

Since the 1990s, the development of modulation schemes in optical fiber communication systems has followed a traditional technical trajectory for single-symbol modulations. This progression encompasses various techniques, including on-off keying (OOK) [1, 2], differential phase-shift keying (DPSK) [3], differential quadrature phase-shift keying (DQPSK) [4], QPSK [5, 6], 16 quadrature amplitude modulation (QAM) [7, 8], 64-QAM [9, 10], and more recently, 4096-QAM. Throughout this evolution, the focus has been on achieving high spectral efficiency (SE) and high-capacity transmissions by increasing the modulation order of each symbol and mitigating the effects of inter-symbol interference (ISI). As the modulation order continues to increase, however, the single-symbol modulation technique faces several challenges, including significant degradation in receiver sensitivity and substantial increase in implementation complexity.

More specifically, Table I presents a chronological summary of research achievements in optical fiber communication systems that utilize single-symbol modulation. The timeline depicted in the table begins in 1999 when Terabit optical communications using OOK modulation were proposed [1]. The table extends to 2020, encompassing the research on dual-polarization (DP) 4096-QAM for achieving higher SE in optical fiber transmissions [16]. Regarding modulation and detection techniques, the key technologies have progressed from intensity modulation direct detection (IMDD) to differential phase modulation direct detection, and subsequently to more comprehensive I/Q modulation and coherent detection. These advancements prioritize symbol orthogonality and strive to eliminate symbol correlations. The table shows sensitivity costs of the modulation formats relative to DP-QPSK, which quantitatively indicates the severe degradation of receiver sensitivity induced by high-order single-symbol modulations. For instance, from the 256-QAM to 4096-QAM, the improvement in SE is only 1.6 times, whereas the cost increase of receiver sensitivity is 35 times, i.e. 15.4 dB.

It is also shown in the table that, coding techniques have also been developed, encompassing both channel coding for forward error correction (FEC) and source coding for symbol probability shaping (PS). These coding techniques aim to enhance receiver sensitivity by introducing redundant parity bits that are correlated with the original information bits. The improvements brought with coding correlations, however,

TABLE I. Single-symbol Modulation Optical Communication Development Path and Research Status

Years	Modulation Format	Spectral Efficiency (b/s/Hz)	Relative Sensitivity Cost (dB)	Key Technologies	Ref.
1999 2003	OOK	0.87	4.3	Direct modulation & direct detection, FEC	[1, 2]
2005	DPSK	0.87	1.3	Differential modulation & direct detection, FEC	[3]
2007	DQPSK	1.74	2.7	Differential modulation & direct detection, FEC	[4]
2008 2009	**DP-QPSK**	**3.5**	**0 (Baseline)**	**I/Q modulation & coherent detection, FEC**	[5, 6]
2010 2011	DP-16QAM	6.2	4.5	I/Q modulation & coherent detection, FEC	[7, 8]
2015 2019	DP-64QAM	8.0	5.1	I/Q modulation & coherent detection, FEC, probabilistic shaping	[9, 10]
2017 2019	DP-256QAM	10.1	9.8	I/Q modulation & coherent detection, FEC, probabilistic shaping	[11, 12]
2018	DP-1024QAM	13.2	15.2	I/Q modulation & coherent detection, FEC, probabilistic shaping	[13, 14]
2019 2020	DP-4096QAM	15.8	25.2	I/Q modulation & coherent detection, FEC, probabilistic shaping	[15, 16]

cannot effectively balance out the sensitivity drop caused by the high-order single-symbol modulations.

One way to overcome the limitations posed by the high-order single-symbol modulations is the use of multi-symbol correlation, which was first proposed for optical fiber nonlinearity compensation in 2010 [17] and latter extended to high SE transmissions [18–20]. Then in 2013 and 2015, the schemes based on duobinary and triple-binary shaping were experimentally demonstrated [21–23], respectively. In 2021 and 2022, we proposed and demonstrated a combined pattern-dependent-equalization (PDE) and look-up-table (LUT) based maximum likelihood sequence estimation (MLSE) scheme for high SE transmissions [24, 25]. By extracting insights from the previous research accomplishments, we synthesize in this paper a new technology pathway called correlated multi-symbol modulation (CMSM) scheme. Unlike conventional single-symbol modulation systems, which typically avoid correlations among symbols due to the introduction of ISI, the CMSM system deliberately introduces symbol correlation to achieve a higher SE. We investigate the pattern-dependent features of the CMSM and incorporate the features into essential digital signal processing algorithms for system implementation.

II. Correlated Multi-symbol Modulation Scheme

As aforementioned, both the CMSM and coding schemes improve receiver sensitivity by inducing symbol correlations. However, the implementation requirements and resulting signal features are different. Coding schemes establish symbol correlations without generating ISI, but at the cost of increased line rate, resulting in reduced SE. On the other hand, CMSM creates symbol correlations by intentionally introducing ISI, leading to improved SE without requiring additional parity overhead like coding schemes.

Fig. 1 depicts the symbol correlations induced at various stages in an optical fiber communication system. Alongside the intentionally induced modulation correlation through carefully designed narrowband filtering, there are modulation correlations that passively arise due to transceiver bandwidth limitations and transmission effects in a practical system implementation. Therefore, when designing a CMSM-based system, the objective is to effectively control and utilize symbol correlations throughout the entire signal processing chain, including modulation, demodulation, sequence detection, and error correction, in order to enhance overall system performance.

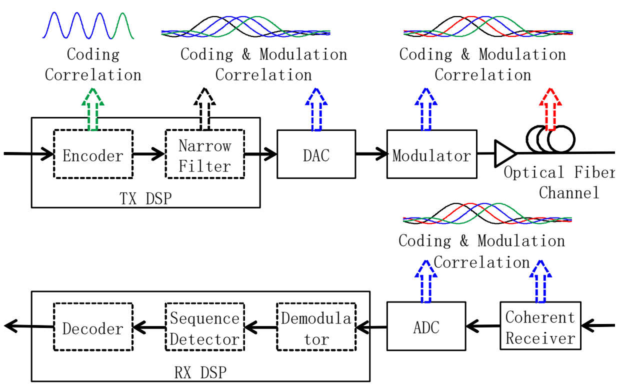

Fig. 1. Symbol modulation correlation and symbol coding correlation.

A particular challenge in CMSM based systems is how to effectively transfer and process accordingly different types of modulation correlations. For instance, the deterministic and data-pattern dependent symbol correlation internationally induced by narrowband filtering needs to be reserved and transferred to the sequence detection module for receiver sensitivity improvement. On the other hand, the symbol correlation induced by dynamic polarization-related effects needs to be distinguished from and equalized off the narrowband filtering correlation.

To resolve the problem, we propose to use a pattern-dependent LUT for symbol correlation features recording, transferring, and processing through the DSP modules. As shown in Fig. 2, an LUT shared by all DSP modules enables system assembling and comprehensive optimization with common knowledge of target modulation correlation features. Figure 2 also indicates that although prior works have applied pattern-dependent LUT to sequence detection, the multi-symbol modulation and demodulation blocks need to replace their counterparts in conventional single-symbol modulation systems to complete the whole puzzle of a CMSM system.

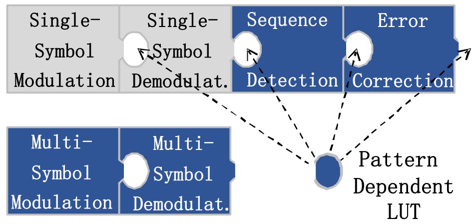

Fig. 2. Proposed CMSM scheme employing a pattern dependent LUT for symbol correlation transferring through DSP modules.

III. Modulation and Demodulation in CMSM System

One straightforward solution for the correlated modulation process in CMSM systems is narrowband filtering, which compresses the signal spectrum by spreading out signal pulses in time domain. The narrowband filtering is implemented in transmitter-side DSP where a pattern-dependent LUT recording the signal correlation features can be generated, namely Tx LUT, to guide the correlated demodulation and sequence detection processes at the receiver. Similar to its counterpart high-order single-symbol modulation, a price to pay for the narrowband filtering is a higher bit resolution in digital to analog conversion (DAC).

As shown in Fig. 3, the demodulation subsystem in a coherent optical transmission system generally performs clock recovery, adaptive equalization, frequency offset compensation (FOC) and carrier phase estimation (CPE). Among these functions, adaptive equalization is the one that is capable to actively shape the symbol correlation features. Two output constellations are depicted in Fig. 3 as examples of correlation changes that can be made by an adaptive equalizer. The two compared scenarios can be alternated with a switch setting that controls the connection between the equalizer and an LUT providing target symbol correlation characteristics. As shown in Fig. 3, the data-pattern LUT can also be generated at the receiver side through training and/or

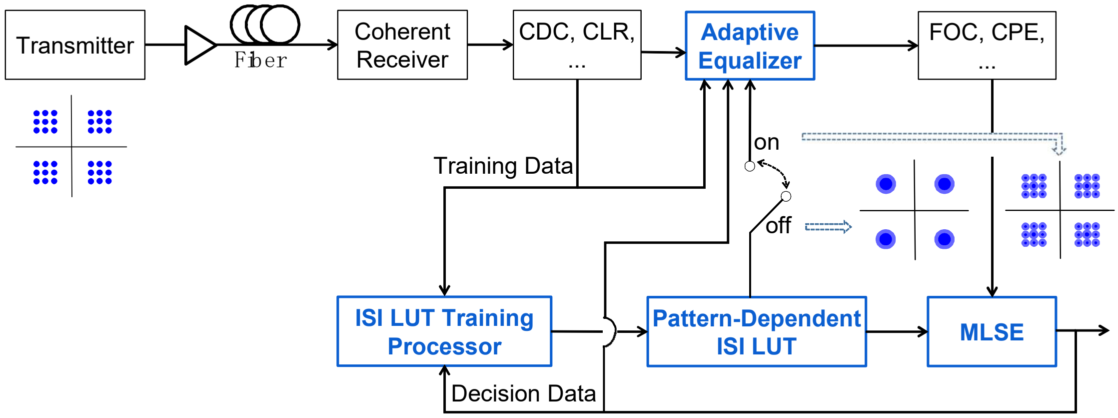

Fig. 3. CMSM transmission system with a PDE and a MLSE sharing a pattern-dependent LUT.

decision feedback, namely Rx LUT. Compared to a Tx LUT, an Rx LUT can characterize symbol correlations induced by system limitations and transmission effects in addition to that induced by the narrowband filtering at transmitter. The added complexity is a tradeoff for improved system performance.

In the switch-off scenario in Fig. 3, the adaptive equalizer operates as a regular CMA equalizer. It calculates the equalization error between the received signal and a constant modulus feature of a regular QPSK signal. The equalizer treats the modulation correlation induced at the transmitter as ISI and eliminates it, resulting in a regular4-spot QPSK constellation. In the switch-on scenario, the equalization process targets at reserving the symbol correlations recorded in the pattern-dependent LUT that is indexed by the symbol or bit patterns of multiple consecutive symbols. Each entry of the LUT contains sample values of the digitized signal segment corresponding to its indexing data pattern. The proposed process of incorporating the LUT in the adaptive equalization is as follows:

1) For polarization h, an index k_h is first needed to calculated as a function of data pattern $\boldsymbol{S}_h$ by

$$k_h = f_1(\{\ldots, S_h^{i-1}, S_h^{i}, S_h^{i+1}, \ldots\}). \quad (1)$$

2) The equalization error e_h is be calculated by selecting a LUT entry $\{\ldots, L_{kh}^{i-1}, L_{kh}^{i}, L_{kh}^{i+1}, \ldots\}$ according to k_h as an input. The e_h is given by

$$e_h = |L_{kh}^{i} - S_h'^{i}|. \quad (2)$$

3) The least mean square (LMS) method is used to iteratively update the coefficients using the calculation error e_h to achieve adaptivity.

As described above, when setting a goal for the adaptive equalization to eliminate as much ISI as possible from the received signal, useful pattern-dependent symbol correlations would be broken together with unwanted ISIs, and thus, the modulation correlations cannot be transferred to the subsequent MLSE. In contrast, the use of LUT-based correlation transfer mechanism in CMSM modulation systems allows the impairing dynamic symbol correlations related to the effects such as polarization mode dispersion (PMD) and polarization state rotation being distinguished and eliminated, and the pattern-dependent deterministic symbol correlations being retained and passed to the subsequent sequence detection module.

IV. Optical Fiber Transmission Experiments with CMSM

Figure. 4 shows the transmission experimental setup of the proposed CMSM system employing combined LUT-based adaptive equalization and MLSE scheme for narrowband filtered QPSK signal. An arbitrary waveform generator (AWG, 20 GHz BW) with a 64 GSa/s sampling rate was used to generate a 32 Gbaud DP-QPSK signal filtered by a 4 GHz (i.e., 1/8 of the baud rate) 1st-order Gaussian filter. A 40 GHz bandwidth coherent driver modulator (CDM) with integrated four parallel differential input linear drivers was used for I/Q modulation. The number of fiber spans was up to 12 with a span length of 80 km.

Figure 5 plots the transmission performance of the CMSM scheme compared against a single-symbol modulation scheme. The experimental results show that at all the distances experimented, ranging from 160 km up to 1040 km, the CMSM scheme achieves Q-factors significantly higher than the conventional single-symbol modulation scheme. In

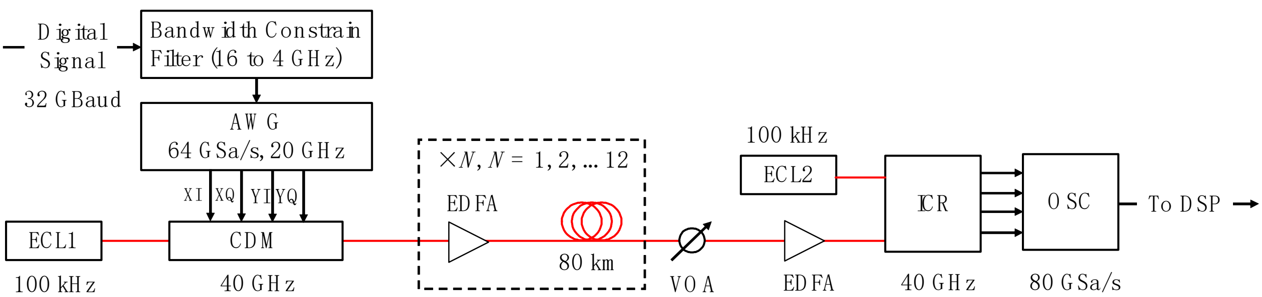

Fig. 4. Transmission experiment setup for verifying the proposed PDE scheme in bandwidth-constrained QPSK signaling scenarios.

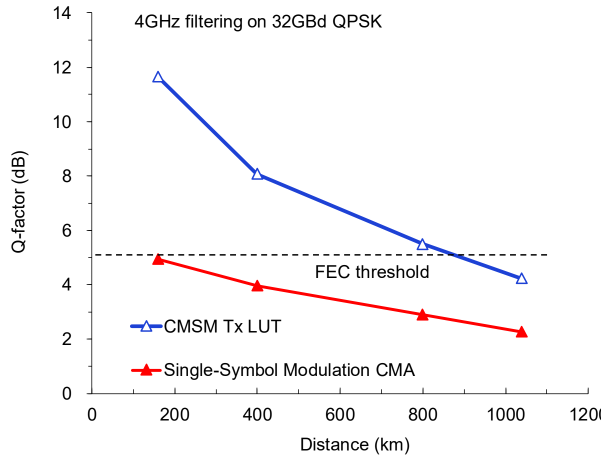

Fig. 5. Transmission performance of the ISI mitigation schemes.

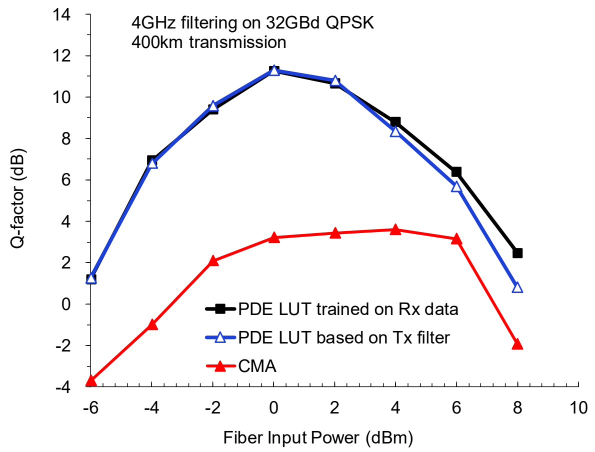

Fig. 6. Transmission performance with different fiber input power.

particular, for an FEC threshold at 5.16 dB Q, the CMSM scheme can achieve 800 km transmission, whereas the conventional scheme fails at 160 km.

To investigate the performance of the CMSM scheme in nonlinear transmission regimes, 400 km transmission experiments with a 4 GHz (1/8 of the baud rate) filtered 32Gbaud DP-QPSK signal were performed with fiber input power ranging from -6 dBm to 8 dBm. The results plotted in Fig. 6 show that the CMSM scheme outperforms the conventional scheme over the whole experimented range of fiber input power. The results show that the CMSM scheme achieves its optimal performance at 0 dBm fiber input power resulting a Q-factor of 11.3 dB, whereas the best Q-factor of the conventional scheme is below 4 dB at its optimal fiber input power setting. It is also observed that compared to the Tx LUT case, employing a Rx LUT achieves similar performance in the linear regimes and slightly better performance in the nonlinear regimes. It shows more advantage as the nonlinearity becomes more severe, indicating that the Rx LUT captured at some of the fiber-nonlinearity-induced correlations and turned these features into a beneficial use.

To investigate the relation between the achievable SE and receiver sensitivity, we performed also back-to-back experiments. Fig. 7 plots the results from the point of view of SE-to-sensitivity cost ratio as a function of SE for a 3-symbol

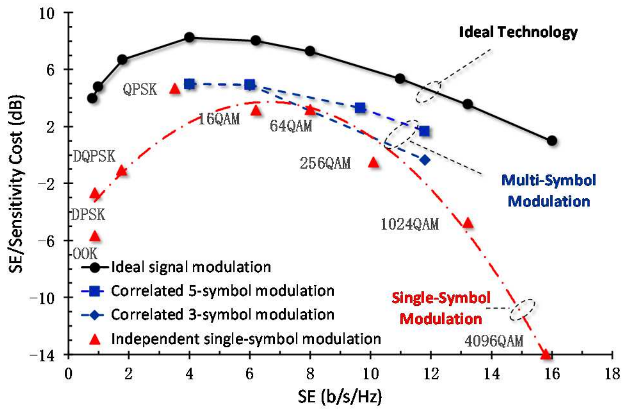

Fig. 7. Technology paths for high SE optical fiber communications

and 5-symbol CMSM systems. For comparison, the SE-to-sensitivity cost ratios of conventional single-symbol QAM modulation schemes, as well as the corresponding theoretical limit derived from the Shannon limit [26], are also shown. The sensitivity costs calculated for generating the curves in Fig. 7 were relative to the DP-QPSK performance listed in Table I. These curves represent three technical paths for improving the SE of optical communication systems at the cost of receiver sensitivity, i.e., single-symbol modulation, CMSM, and ideal technology paths.

Comparing these paths, it can be seen that the SE-to-sensitivity cost ratio of the single-symbol modulation scheme changes parabolically as the modulation order increases. After getting to its highest point at the DP-QPSK modulation format, the single-symbol modulation curve drops more quickly than the other curves, and thus, moving away from rather than getting closer towards the ideal technology path. On the other hand, the CMSM scheme can approach the theoretical limit by generating more correlated symbols in its process. For example, it shows an SE-to-sensitivity cost ratio of -0.33 dB at 11.8 b/s/Hz with 3-symbol CMSM, whereas at the same SE, an SE-to-sensitivity cost ratio of 1.67 dB is achieved with 5-symbol CMSM, demonstrating 2 dB improvement.

V. Conclusion

In this paper, we reviewed the progress of conventional single-symbol modulation technology and showed its limitations in balancing SE and receiver sensitivity. We investigated the potential utilization of modulation correlations in addition to conventional coding correlations for better tradeoffs between SE and receiver sensitivity. Consequently, we proposed a new technology path, namely CMSM, which transforms impairing ISIs in conventional single-symbol modulation systems into beneficial symbol correlations for high SE transmissions. We developed a DSP system structure and corresponding algorithms centered around a common pattern-dependent LUT, facilitating the systematic utilization of modulation correlations. To evaluate the performance of the CMSM system, we conducted optical fiber transmission experiments and demonstrated its significant outperformance compared to the conventional single-symbol modulation system in both linear and nonlinear regimes. By generating more correlated symbols in its process, we showed that the CMSM system holds great promise as a technology path to achieve high SE optical communications that approach the theoretical limits.

ACKNOWLEDGMENT

This work is supported in part by National Key Research and Development Program of China ((2022YFB2903000); National Natural Science Foundation of China (NSFC) (62250710164, 62275185).

REFERENCES

[1] A. Chraplyvy, “Terabit optical communications,” *ECOC' 1999*, paper MoC2.1., Nice, France, Sep. 1999.

[2] Y. Cai, J. M. Morris, T. Adali, and C. R. Menyuk, “On turbo code decoder performance in optical fiber communication systems with dominating ASE noise,” *IEEE/OSA Journal of Lightwave Technology*, vol. 21, no. 3, pp. 727–734, Mar. 2003.

[3] J. Cai, D. Foursa, C. Davidson, L, Liu, Y. Cai, W. Patterson, A. Lucero, B. Bakhshi, G. Mohs, P. Corbett, V. Gupta, W. Anderson, M. Vaa, G. Domagala, M. Mazurczyk, H. Li, S. Jiang, M. Nissov, A. Pilipetskii, and N. Bergano, “RZ-DPSK field trial over 13100 km of installed non-slope-matched submarine fibers,” *IEEE/OSA Journal of Lightwave Technology*, vol. 23, no. 1, pp. 95–103, Jan. 2005.

[4] A. H. Gnauck, C. R. Doerr, P. J. Winzer, S. Cabot, M. A. Cappuzzo, E. Y. Chen, A. Wong-Foy, L. T. Gomez, M. T. Santo, T. Kawanishi, and T. Sakamoto, “Optical equalization of 42.7-Gbaud band-limited NRZ-DQPSK signals for high-spectral-efficiency transmission,” *OFC' 2007*, paper OThN4, Anaheim, California, Mar. 2007.

[5] Y. Cai, “Coherent detection in long-haul transmission systems,” *OFC' 2008*, Invited Paper OTuM1, San Diego, California, Feb. 2008.

[6] K. Roberts, M. O'Sullivan, K. Wu, H. Sun, A. Awadalla, D. Krause, and C. Laperle, “Performance of dual-polarization QPSK for optical transport systems,” *IEEE/OSA Journal of Lightwave Technology*, vol. 27, no. 16, pp. 3546–3559, Aug. 2009.

[7] P. Winzer, A. Gnauck, C. Doerr, M. Magarini, and L. Buhl, “Spectrally efficient long-haul optical networking using 112-Gb/s polarization-multiplexed 16-QAM,” *IEEE/OSA Journal of Lightwave Technology*, vol. 28, no. 4, pp. 547–556, Feb. 2010.

[8] K. Schuh, F. Buchali, D. Roesener, E. Lach, O. Bertran-Pardo, J. Renaudier, G. Charlet, H. Mardoyan, and P. Tran, “15.4 Tb/s transmission over 2400 km using polarization multiplexed 32-Gbaud 16-QAM modulation and coherent detection comprising digital signal processing,” *ECOC' 2011*, paper We.8.B.4, Geneva, Switzerland, Sep. 2011.

[9] F. Buchali, G. Böcherer, W. Idler, L. Schmalen, P. Schulte, and F. Steiner, “Experimental demonstration of capacity increase and rate-adaptation by probabilistically shaped 64-QAM,” *ECOC' 2015*, Post-Deadline Paper PDP.3.4, Valencia, Spain, Sep. 2015.

[10] H. Chien, J. Yu, Y. Cai, B. Zhu, X. Xiao, Y. Xia, X. Wei, T. Wang, Y. Chen, “Approaching Terabits per Carrier Metro-Regional Transmission Using Beyond-100GBd Coherent Optics with Propabilistically Shaped DP-64QAM Modulation,” *IEEE/OSA Journal of Lightwave Technology*, vol. 37, no. 8, pp. 1751–1755, Apr. 2019.

[11] H. Chien, J. Yu, Y. Cai, J Zhang, X Li, and X. Xiao, “400G-over-80km Connections Powered by Probabilistically Shaped PM-256QAM Wavelengths at 34 GBaud,” *ECOC' 2017*, paper P2.SC6.17, Gothenburg, Sweden, Sep. 2017.

[12] A. Matsushita, M. Nakamura, F. Hamaoka, and Y. Kisaka, “41-Tbps C-band transmission with 10-bps/Hz spectral efficiency using 1-Tbps 96-GBd PS-256QAM for DCI,” *ECOC' 2019*, paper Tu2D1, Dublin, Ireland, Sep. 2019.

[13] H. Hu, M. Y.ankov, F. Da Ros, Y. Amma, Y. Sasaki, T. Mizuno, Y. Miyamoto, M. Galili, S. Forchhammer, L. Oxenløwe, and T. Morioka, “Ultrahigh-Spectral-Efficiency WDM/SDM Transmission Using PDM-1024-QAM Probabilistic Shaping With Adaptive Rate,” *IEEE/OSA Journal of Lightwave Technology*, vol.. 36, no. 6, pp. 1304–1308, Mar. 2018.

[14] J. Shi, J. Zhang, N. Chi, Y. Cai, X. Li, Y. Zhang, Q. Zhang, J. Yu, “Probabilistically Shaped 1024-QAM OFDM Transmission in an IM-DD System,” *OFC' 2018*, paper W2A.44, San Diego, CA, March 2018.

[15] X. Chen, S. Chandrasekhar, J. Cho, and P. Winzer, “Transmission of 30-GBd polarization multiplexed probabilistically shaped 4096-QAM over 50.9-km SSMF”, *OSA Optics Express*, vol. 27, no. 21, pp. 29916–29923, Oct. 2019.

[16] X. Chen, J. Cho, and D. Che, “Experimental quantification of implementation penalties from laser phase noise for ultra-high-order QAM signals,” *ECOC' 2020*, paper Tu2D-5, Brussels, Belgium, Dec. 2020.

[17] Y. Cai, D. Foursa, C. Davidson, J. Cai, O. Sinkin, M. Nissov, and A. Pilipetskii, “Experimental demonstration of coherent MAP detection for nonlinearity mitigation in long-haul transmissions,” *OFC' 2010*, Paper OTuE1, San Diego, California, Mar. 2010.

[18] Y. Cai, J. Cai, C. Davidson, D. Foursa, A. Lucero, O. Sinkin, A. Pilipetskii, G. Mohs, N. Bergano, “High spectral efficiency long-haul transmission with pre-filtering and maximum a posteriori probability detection,” *ECOC' 2010*, Invited Paper We.7.C.4, Torino, Italy, Sep. 2010.

[19] J. Cai, Y. Cai, C. Davidson, D. Foursa, A. Lucero, O. Sinkin, W. Patterson, A. Pilipetskii, G. Mohs, N. Bergano, “Transmission of 96 × 100-Gb/s bandwidth-constrained PDM-RZ-QPSK channels with 300% spectral efficiency over 10610 km and 400% spectral efficiency over 4370 km,” *IEEE/OSA Journal of Lightwave Technology*, vol. 29, no. 4, pp. 491–498, 2011.

[20] G. Colavolpe, T. Foggi, A. Modenini, and A. Piemontese, “Faster-than-Nyquist and beyond: how to improve spectral efficiency by accepting interference,” *OSA Optics Express*, vol. 19, no. 27, pp. 26600-26609, Dec. 2011.

[21] J. Yu, J. Zhang, Z. Dong, Z. Jia, H. Chien, Y. Cai, X. Xiao, and X. Li, “Transmission of 8x 480-Gb/s super Nyquist-filtering 9-QAM-like signal at 100 GHz-grid over 5000-km SMF-28 and 25 100GHz-grid ROADMs,” *OSA Optics Express*, vol. 21, no. 13, pp. 15686–15691, July 2013.

[22] I. Darwazeh, T. Xu, T. Gui, Y. Bao, and Z. Li, “Optical SEFDM system; bandwidth saving using non-orthogonal sub-carriers,” *IEEE Photonics Technology Letters*, vol. 26, no. 4, pp. 352–355, Feb. 2014.

[23] Y. Cai, Z. Jia, H. Chien, J. Zhang, and J. Yu, “Bandwidth constraining and digital signal processing for high spectral efficiency optical fiber transmissions,” *OECC' 2015*, Invited Paper JTuA.31, Shanghai, China, June 2015.

[24] Y. Cai, H. Chien, M. Xiang, Z. Hu, and M. Gao, “Adaptive pattern-dependent equalization for coherent optical fiber communication systems,” *OFC' 2021*, Invited Paper F4D.3, San Francisco, California, June 2021.

[25] Y. Cai, H. Chien, M. Xiang, W. Wang, F. Li, Z. Hu, M. Gao, C. Jiang, Z. Tian, H. Xu, K. Zhang, J. Shen, and J. Huang, “Combined symbol-pattern-dependent adaptive equalization and sequence detection for coherent optical fiber communications,” *IEEE/OSA Journal of Lightwave Technology*, vol. 40, no. 5, pp. 1320–1329, Mar. 2022.

[26] C. Shannon, “A mathematical theory of communication,” *The Bell System Technical Journal*, vol. 27, pp. 379–423, 623–656, Oct. 1948.